

CALIBRATION OF 2D HYDRAULIC INUNDATION MODELS IN THE FLOODPLAIN REGION OF THE LOWER TAGUS RIVER

Pestana, R. ⁽¹⁾, Matias, M. ⁽¹⁾, Canelas, R. ⁽¹⁾, Araújo, A. ⁽¹⁾, Roque, D. ⁽²⁾, Van Zeller, E. ⁽³⁾, Trigo-Teixeira, A. ⁽¹⁾, Ferreira, R. ⁽¹⁾, Oliveira, R. ⁽¹⁾, Heleno, S. ⁽¹⁾

⁽¹⁾ Instituto Superior Técnico, Av. Rovisco Pais 1, Lisbon (Portugal);
email:rita.pestana@ist.utl.pt;sandra.heleno@ist.utl.pt

⁽²⁾ Laboratório Nacional de Engenharia Civil, Av. Brasil, Lisbon (Portugal);

⁽³⁾ Agência Portuguesa do Ambiente, Av. Gago Coutinho, Lisbon (Portugal);

ABSTRACT

In terms of inundated area, the largest floods in Portugal occur in the Lower Tagus River. On average, the river overflows every 2.5 years, at times blocking roads and causing important agricultural damages. This paper focus on the calibration of 2D-horizontal flood simulation models for the floods of 2001 and 2006 on a 70-km stretch of the Lower Tagus River. Flood extent maps, derived from ERS SAR and ENVISAT ASAR imagery were compared with the flood extent maps obtained for each simulation, to calibrate roughness coefficients. The combination of the calibration results from the 2001 and 2006 floods provided a preliminary Manning coefficient map of the study area.

1. INTRODUCTION

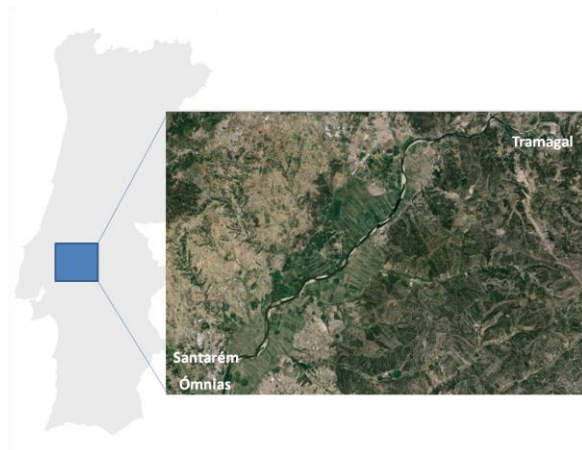


Figure 1. Location of the study area, a 70-km stretch of the Lower Tagus River, Portugal, between Tramagal and Ómnias.

Floods are one of the most deadly natural hazards worldwide, and the deadliest in Portugal in the last 100 years. In terms of inundated area, the largest floods in Portugal occur in the Lower Tagus River (Fig. 1). On average, the river overflows every 2.5 years, at times

blocking roads and causing important agricultural damages. The economical relevance of the area and the high frequency of the relevant flood events make the Lower Tagus floodplain a good pilot region to conduct a data-driven calibration of flood hydraulic models.

In this study we use flood extent maps, derived from ERS SAR and ENVISAT ASAR imagery, to calibrate 2D horizontal flood simulation models for two floods that occurred on the Lower Tagus River (in January 2001 and November 2006) in order to obtain a 100 m resolution manning's coefficient map.

2. DATA AND METHODS

For the hydraulic simulations we used the commercial software TufLOW, which provides 2D solutions based on the Stelling finite-difference, alternating direction implicit (ADI), scheme that solves the full 2D free surface shallow-water flow equations. The model allows the introduction of 1D and 2D structures that constrain water flow, such as dykes. The medium it uses is water and the grid is structured. We can introduce boundary conditions: flow upstream and water level downstream.



Figure 2. Detail of the DTM used in the simulations

The hydraulic models used a 5m-resolution digital terrain model (Fig.2) acquired by Intermap ©. The DTM was obtained with IFSAR Technology during a dry period (in March/April 2008), which allowed a

better definition of the margins of the river, islets and sand banks [1].

In-situ measurements of water elevation in Omnias (downstream boundary condition) and discharge flow in Tramagal (upstream boundary condition) were available for the simulations (see locations in Fig. 1). Due to the relevancy of several dykes on this stretch of the LT River, non-existent on the available DTM, five of them were introduced in the models. All model runs had the same boundaries and were simulated using steady-state flow initial conditions. The resolution of the 2D grid mesh was 30m.

Flood extent maps, derived from ERS SAR and ENVISAT ASAR imagery, provided spatially distributed data for calibration of the hydraulic models. The flood extent maps obtained for each simulation were compared with the flood extent maps derived from SAR imagery and the roughness coefficients were adjusted accordingly. Different measures of the similarity between simulated and imaged flood extents (overall accuracy, kappa coefficient and omission and commission errors) were derived from confusion matrices using the software ENVI. The models were also calibrated in terms of the stage at the gauge station Almourol, located 12km downriver from Tramagal.

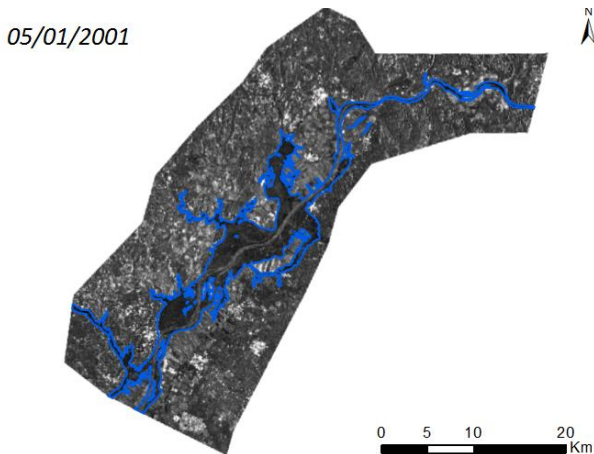


Figure 3a. ERS SAR image acquired during the flood of January 2001 and delimitation of flooded area (in blue)

Fig. 3a and b show Synthetic Aperture Radar (SAR) images for the flood of January 2001 and for the flood of November 2006, respectively. The darker regions represent water. Two methods were used for the delimitation of the flooded area: visual interpretation followed by manual delimitation, and an object-based supervised automated method [2]. The flood delimitation assisted by visual interpretation is represented in blue in the figures.

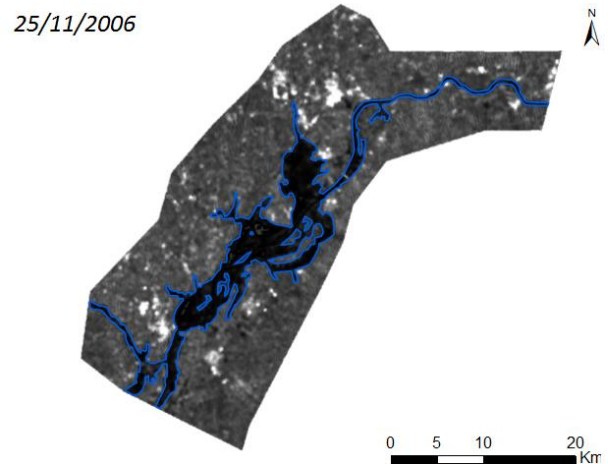


Figure 3b. ASAR Wide Swath image acquired during the flood of November 2006

Land cover data for the study area was retrieved from Corine Land Cover 2006 (CO-ordination of INformation on the Environment) with spatial resolution of 100m. Since there are no roughness coefficient values defined for our study area, the initial roughness coefficient map used in the simulations was based on the Corine Land Cover classes, crossed with roughness coefficient values in the literature for other study areas (e.g. [3][4][5][6]). The most common Corine Land Cover classes on the Lower Tagus River floodplain are the agricultural areas. The most frequent is the class 212 (the permanently irrigated land). Another one is the 221 (vineyards). For the class pastures (231), for example, we found different values in the literature. On these cases we opted to use the medium value. Also, for some of the classes we did not find equivalent classes on the literature, so we opted to use the default value of 0.05 for the manning coefficient.

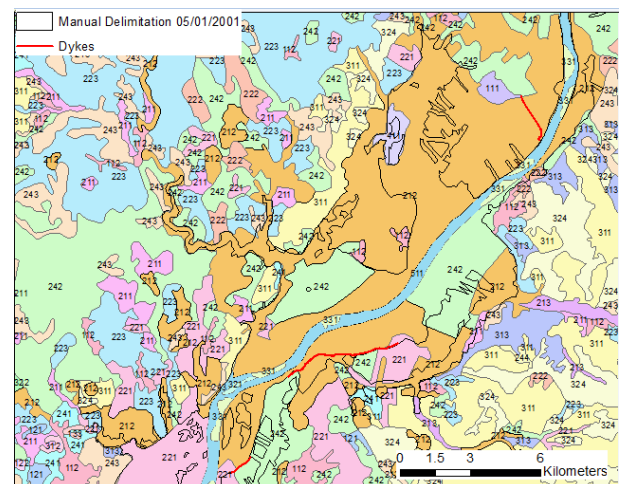


Figure 4. Detail of Corine LC classes in the floodplain, and delimitation of the January 2001 flood

A detail of Corine Land Cover classes in the floodplain is depicted in Fig. 4, superimposed by the delimitation of the flood of January 2001 (black contour). The figure illustrates the fact that only a few land cover classes (212, 221, 242) are present in the floodplain. These were the classes chosen for the adjustment of the manning coefficient values.

Fig. 5 depicts the downstream boundary condition of water level in Ómnias for the simulations of the flood of January 2001. The peak flow discharge in Tramagal (upstream boundary condition) was 4675m³/s. We ran the simulation from 5pm of 29/12/2000 until 1am of 9/01/2001. The ERS-2 SAR image, with pixel dimensions of 12.5 meters, was acquired at 11pm of 5/01/2001.

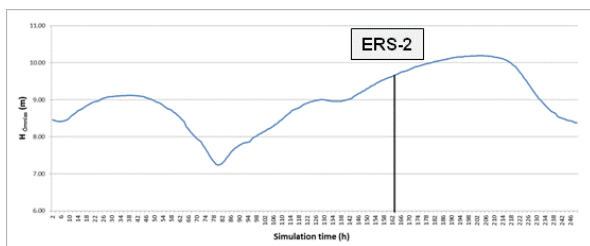


Figure 5. Downstream water level for the simulations of the January 2001 flood and ERS-2 acquisition

Fig. 6 shows the water level in Ómnias (downstream boundary condition) for the simulation of the November 2006 flood. The peak flow discharge in Tramagal (upstream boundary condition) was 3266m³/s. We ran the simulation from 12pm of 18/11/2006 until 12 am of 3/12/2006. The ENVISAT ASAR WS image has pixel

dimensions of 75 meters.

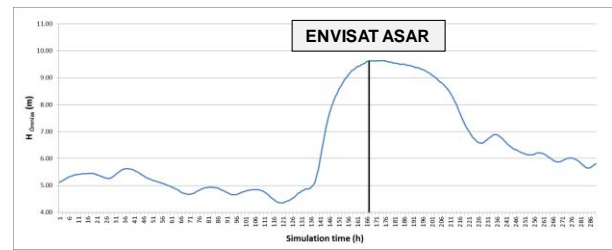


Figure 6. Downstream water level for the simulations of the November 2006 flood and ASAR acquisition

3. RESULTS AND DISCUSSION

Tab. 1 summarizes the calibration results for several simulations performed for the January 2001 flood, with the respective measures of the similarity between simulated and imaged flood extents: overall accuracy, kappa coefficient and omission and commission errors. Besides adjusting the manning coefficient values individually for some classes, we also changed the manning values jointly for all classes in order to assess the model's response (examples in blue and yellow in Tab. 1).

Fig. 7 illustrates the flood extents resulting from the decrease of 30% in the manning coefficient values (for all classes, see the blue line in Tab. 1) and from an increase of 15% (yellow line in the same table) in the manning values. We can see that the increase on the manning coefficient n causes the increase of the flooded area.

Manning Coefficient						overall	k	omission	comission
212	221	242	511	512	...	accuracy (%)	coefficient	(%)	(%)
0.200	-	-	-	-	-	96.15	0.77	15.93	24.63
0.015	-	-	-	-	-	95.86	0.73	27.98	20.54
-	0.200	-	-	-	-	95.98	0.75	22.00	22.95
-	0.015	-	-	-	-	96.12	0.75	24.37	20.34
-	-	0.200	-	-	-	95.73	0.74	23.79	24.22
-	-	0.015	-	-	-	96.13	0.76	23.37	20.92
-	-	-	0.020	0.020	-	96.25	0.74	32.83	12.30
-	-	-	0.040	0.040	-	95.71	0.76	13.50	28.69
-	-	-	0.050	0.050	-	94.96	0.73	9.51	34.29
0.100	-	-	0.020	0.020	-	96.33	0.75	30.91	13.13
0.150	-	-	0.025	0.025	-	96.46	0.78	22.56	18.25
-30.00%						96.20	0.73	37.12	8.37
15.00%						95.74	0.75	16.46	27.37
30.00%						95.43	0.75	11.68	31.08
0.015	30.00%					95.90	0.72	32.40	16.97
-						96.10	0.76	23.52	21.11
0.050						94.76	0.66	32.26	30.42

Table 1. Calibration results for several simulations performed for the January 2001 flood, and measures of the similarity between simulated and imaged flood extents

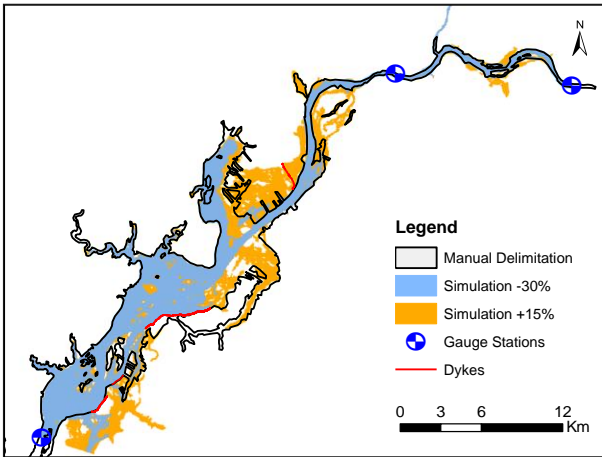


Figure 7. Flood extents resulting from the decrease of 30% in the manning values (blue) and from an increase of 15% (yellow), and manual delimitation of the 2001 flood extent countoured in black

We interpreted the measures of the similarity between simulated and imaged flood extents as a whole. The omission errors measure the areas that appear flooded on the SAR image, but not on the simulated maps. The commission errors measure the areas that appear flooded on the simulation but not on the SAR image. We used the criteria of prioritizing the reduction of the omission errors as these results will be used to produce hazard maps. So, for the flood of January 2001, the best simulated result was obtained when the manning coefficient value was changed individually for the class 212 to $n=0.20$. For this case the omission (15.93%) and commission (24.63%) errors are relatively low, and the overall accuracy is high (96.15%). Also the kappa coefficient is relatively high (0.77). Fig. 8 shows the omission/commission errors for this best case.

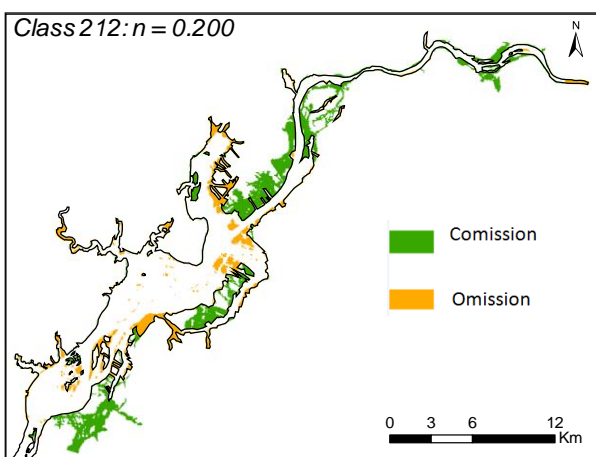


Figure 8. Omission and commission errors for the best case simulation of the January 2001 flood

The same calibration process was repeated for the November 2006 flood, and comparing the results from both floods, we concluded that an increase of 15% in the manning coefficient values (for all classes) resulted in the best measures of similarity between simulated and imaged flood extents. Figs. 9a and b display these best case simulations for January 2001 and November 2006 floods, respectively, and the measures of similarity are presented in Tab. 2.

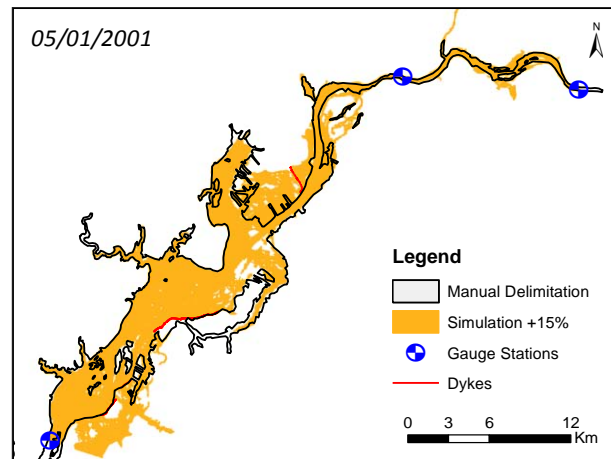


Figure 9a. January 2001 simulated flood extent resulting from the increase of 15% in the Manning values and comparison with the manual delimitation on the SAR image

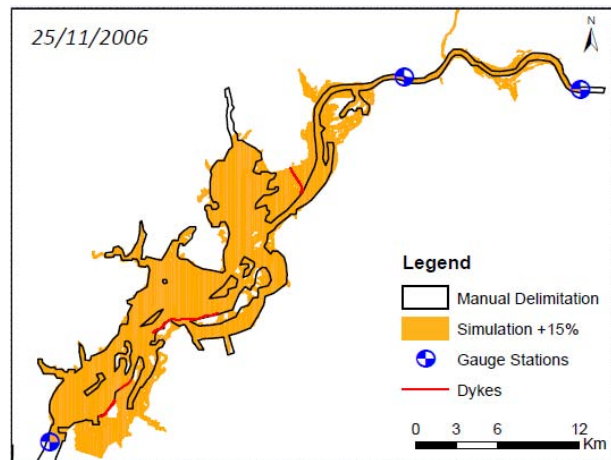


Figure 9b. November 2006 simulated flood extent resulting from the increase of 15% in the Manning values and comparison with the manual delimitation on the SAR image

	overall	k	omission	comission
Flood	accuracy (%)	coefficient	(%)	(%)
05-01-2001	95.74	0.75	16.46	27.37
25-11-2006	95.60	0.78	8.09	29.08

Table 2. Measures of similarity with manual delimitations, for the two flood simulations in Fig.9

Code	Designation	n
111	Continuous urban fabric	0.230
112	Discontinuous urban fabric	0.115
121	Industrial or commercial units	0.230
122	Roads and rail networks and associated land	0.038
124	Airports	0.230
131	Mineral extraction sites	0.104
132	Dump sites	0.115
133	Construction sites	0.115
142	Sport and leisure facilities	0.023
211	Non-irrigated arable land	0.043
212	Permanently irrigated land	0.043
213	Rice fields	0.023
221	Vineyards	0.043
222	Fruit trees and berry plantations	0.043
223	Olive groves	0.043
231	Pastures	0.298
241	Annual crops associated w/permanent crops	0.043
242	Complex cultivation patterns	0.023
243	Agriculture, w/significant natural vegetation	0.058
244	Agro-forestry areas	0.058
311	Broad-leaved forest	0.230
312	Coniferous forest	0.127
313	Mixed forest	0.230
321	Natural grasslands	0.039
322	Moors and heathland	0.058
323	Sclerophyllous vegetation	0.058
324	Transitional woodland-shrub	0.058
331	Beaches, dunes, sands	0.138
332	Bare rocks	0.104
333	Sparsely vegetated areas	0.104
334	Burnt areas	0.104
411	Inland marshes	0.115
511	Water courses	0.035
512	Water bodies	0.035

Table 3. Roughness coefficient values for the Corine Land Cover classes on the Lower Tagus River area

Tab. 3 presents our preliminary roughness coefficient values for the Corine Land Cover classes on the Lower Tagus River area. These were used to build a roughness coefficient map, but we need to safeguard the following: n depends on the flow peak discharge of each flood, as shown in this study; there are errors associated with the DTM, as it was collected in 2008 and our floods occurred in 2001 and 2006; we have different resolution for the SAR images, which can introduce errors on the delimitation; and the calibration of n allows to compensate for other uncertainties on the simulation process.

4. CONCLUSIONS AND FUTURE WORK

Tuflow software successfully models floods on the study area (70-km stretch of the Lower Tagus river). Our findings show that roughness coefficient values matter: we saw that small changes in one land cover class manning value may significantly alter the

simulation results. We were able to find a best case roughness coefficient map for the Corine Land Cover classes on the Lower Tagus River area.

In future work we intend to increase the grid resolution of the model mesh; calibrate the roughness coefficients for two more floods (November 1997 and February 2001); and use the final roughness coefficient map thus obtained to perform simulations for different flood hydrometric scenarios and cross these results with cartographic and land use information, hence contributing to flood hazard mapping in the Tagus River Basin.

5. REFERENCES

1. Matias, M.P., Falcão, A.P., Gonçalves, A.B., Alvares, T., Pestana, R., Van Zeller, E., Rodrigues, V., & Heleno, S. (this volume). A methodology to generate a digital elevation model by combining topographic and bathymetric data in fluvial environments. *Proceedings of the ESA Living Planet Symposium, Edinburgh September 9-13, 2013*.
2. Roque, D., Afonso, N., Fonseca, A.M. & Heleno, S. (this volume). Building a database of flood extension maps using satellite imagery. *Proceedings of the ESA Living Planet Symposium, Edinburgh September 9-13, 2013*.
3. De Roo, A.P.J. (1999). LISFLOOD: a rainfall-runoff model for large river basins to assess the influence of land use changes on flood risk. In Balabanis, P. et al. (Eds.), *Ribamod: River Basin Modelling, Management and Flood Mitigation*. Concerted Action, European Commission.
4. Kalyanapu, A., Burian, S. & McPherson, T. (2009). Effect of land use-based surface roughness on hydrologic model output. *Journal of Spatial Hydrology*, **9**(2).
5. Kotani, M., Imamura F. & Shuto., N. (1998). Tsunami run-up simulation and damage estimation by using GIS. *Proc. of Coastal Eng., JSCE*, **45** (1), pp. 356–360.
6. Mattocks, C., Forbes, C & Ran, L. (2006). Design and Implementation of a Real-Time Storm Surge and Flood Forecasting Capability for the State of North Carolina, UNC-CEP Technical Report. November 30, 2006.

6. ACKNOWLEDGEMENTS

We thank the Foundation for Science and Technology (FCT) for funding the project RIVERSAR (PTDC/CTE-GIX/099085/2008), and SNIRH for making the hydrometric data available. Data provided by ESA through category-1 projects 9441 and 11576.